International Journal of Science and Research (IJSR)
ISSN: 2319-7064
Impact Factor 2024: 7.101

Analytical Investigation of Solute Dispersion in Combined Free-Forced Convective Flow with Wall Absorption and Bulk Chemical Reaction

Nayan Biswas

Assistant Professor, Department of Mathematics, Nabagram Hiralal Paul College
Email: *nayan[at]hiralalpaulcollege.ac.in*

Abstract: ***This study presents an analytical investigation of solute dispersion phenomena in a fully developed laminar free and forced convective flow between two parallel plates, incorporating the simultaneous effects of wall absorption and bulk chemical reaction. The Mei multi-scale homogenization method is employed to derive closed-form analytical solutions of the convective–diffusion equation under a uniform temperature gradient along the channel walls. The influence of the Grashof number*** (G)***, representing buoyancy effects, on Taylor dispersivity, longitudinal, and transverse concentration distributions is comprehensively analyzed for both heating*** $(G > 0)$ ***and cooling*** $(G < 0)$ ***conditions. The results reveal that Taylor dispersivity remains identical for positive and negative values of the Grashof number, highlighting the symmetric influence of buoyancy on the overall dispersion process. It is observed that longitudinal solute concentration decreases with increasing buoyancy, while transverse concentration distribution exhibits an inverse behavior. Furthermore, boundary absorption and bulk chemical reaction are found to significantly reduce solute dispersivity, leading to attenuation of tracer concentration near reactive surfaces. Validation with existing analytical results demonstrates excellent agreement for the convective component of the dispersion coefficient. The outcomes of this research provide valuable insights into coupled convective–diffusive–reactive transport mechanisms, with potential implications for chemical process design, nuclear waste management, environmental pollution control, and biofluid engineering systems.***

Keywords: Free and forced convection, Taylor dispersivity, Grashof number, Boundary absorption, Bulk chemical reaction, Multi-scale homogenization, Solute transport, Convective–diffusive flow, Reactive walls, Environmental fluid mechanics

1. Introduction

The study of solute dispersion in convective fluid flow systems has gained significant attention due to its extensive applications in various engineering, environmental, and biomedical processes. Solute transport in fluid mediums governs crucial operations such as pollutant migration in natural water bodies, nutrient distribution in biological tissues, and chemical mixing in industrial reactors. In particular, understanding the combined effects of convection, diffusion, and chemical reaction mechanisms plays a fundamental role in improving the design and efficiency of systems used in nuclear waste management, chemical process industries, and environmental remediation technologies [1]–[3].

The concept of dispersion in laminar flow was first introduced by Taylor [4], who demonstrated that solute spreading along the flow direction results from the interplay between molecular diffusion and shear-induced velocity gradients. Later, Aris [5] refined the theory by introducing the concept of *effective dispersion coefficient*, which quantifies the enhanced mixing rate in laminar conduits. Subsequent studies extended this framework to different flow geometries and reactive boundaries, revealing the complex coupling between hydrodynamics and solute transport [6],[7].

In real-world applications, convective transport often involves simultaneous free and forced convection, where buoyancy forces induced by temperature gradients interact with pressure-driven flow. The ratio of buoyancy to viscous forces is characterized by the Grashof number (G), which significantly affects the velocity profile and dispersion characteristics of the solute [8]. Positive values of G correspond to heating of the channel walls, while negative values represent cooling effects. The impact of G on solute dispersion is of particular importance in thermal-fluid systems such as solar collectors, heat exchangers, and nuclear reactors [9],[10].

In addition to buoyancy-driven effects, the role of wall absorption and bulk chemical reaction further complicates the dispersion process. Reactive boundaries introduce additional sink terms that reduce solute concentration near channel walls, altering both longitudinal and transverse dispersion patterns [11],[12]. Gupta and Gupta [13] demonstrated that first-order chemical reactions reduce Taylor dispersivity, while Mazumder and Das [14] reported that wall absorption causes deviation from Gaussian concentration profiles due to enhanced solute depletion. These interactions are crucial in systems involving catalytic surfaces, chemical reactors, and biomedical transport phenomena.

To analytically capture the multi-scale nature of these transport processes, Mei and Vernescu [15] developed the *multi-scale homogenization method*, an asymptotic technique that separates fast and slow time scales to derive upscaled equations for macroscopic solute dispersion. This method has proven to be highly effective in modeling solute transport in heterogeneous and reactive flow systems [16],[17]. Recent studies have successfully applied this framework to magnetohydrodynamic (MHD) flows, porous media, and reactive channels, demonstrating its versatility in complex fluid environments [18]- [20].

The present work extends these studies by analytically investigating solute dispersion in a combined free and forced convective flow between two parallel plates in the presence

of wall absorption and bulk chemical reaction. The Mei multi-scale homogenization method is utilized to derive closed-form analytical solutions to the convective–diffusion equation under a uniform temperature gradient. Special emphasis is placed on examining the role of the Grashof number in modifying the Taylor dispersivity, as well as the longitudinal and transverse concentration distributions, under both heating ($G > 0$) and cooling ($G < 0$) conditions. The study also validates its theoretical predictions with existing models, ensuring consistency and reliability.

The findings presented herein are expected to contribute to the deeper understanding of coupled convective–diffusive–reactive mechanisms, which are vital for optimizing chemical reactor design, controlling pollutant dispersion, and improving heat and mass transfer efficiency in advanced thermal-fluid systems.

2. Mathematical Formulation

In this section, a comprehensive mathematical model is developed to analyze magnetohydrodynamic (MHD) reactive flow and solute dispersion of a viscous, incompressible, and electrically conducting fluid between two parallel vertical plates. The flow is influenced simultaneously by magnetic field, buoyancy, and first-order chemical reaction effects.

2.1 Physical Model and Flow Assumptions

Consider a fully developed, steady, laminar MHD flow of an incompressible fluid between two infinite vertical plates separated by a distance $2h$. The $x^* -$ axis is taken vertically along the channel, and the $y^* -$ axis is normal to it.

The flow is driven by both pressure gradient and buoyancy effects, with a transverse magnetic field B_0 applied perpendicular to the plates. A uniform temperature gradient is imposed along the channel walls, and solute is released from an instantaneous point source within the fluid domain.

Assuming no induced magnetic field and small magnetic Reynolds number, the governing equations are simplified using the Boussinesq and Ohmic approximations.

2.2 Governing Equations of Motion

For steady, fully developed flow, the momentum equation in the $x^* -$ direction is written as:

$$\mu\frac{d^2u^*}{dy^{*2}} - \frac{dp^*}{dx^*} + \rho_0 g\alpha(T^* - T_\infty) - \sigma B_0^2 u^* = 0\,, \quad (1)$$

where $\mu =$ dynamic viscosity, $\rho_0 =$ reference density, $g =$ gravitational acceleration, $\alpha =$ thermal expansion coefficient, $B_0 =$ magnetic field intensity, $\sigma =$electrical conductivity, T^* and $T_\infty =$local and ambient temperatures, respectively.

The temperature field under a uniform axial temperature gradient is expressed as:

$$T^* - T_\infty = Nx^* + \psi^*(y^*)\,, \quad (2)$$

where N represents the imposed temperature gradient and $\psi^*(y^*)$ denotes the transverse temperature variation.

Under the Boussinesq approximation, the density variation is:

$$\rho = \rho_0[1 - \alpha(T^* - T_\infty)]\,. \quad (3)$$

Substituting Eq. (3) into the momentum equation (1) gives:

$$\mu\frac{d^2u^*}{dy^{*2}} - \frac{dp^*}{dx^*} - \rho_0 g\alpha\left(Nx^* + \psi^*(y^*)\right) - \sigma B_0^2 u^* = 0\,. \quad (4)$$

2.3 Non- Dimensionalization

Introducing the following dimensionless variables:

$$y = \frac{y^*}{h}\,, u = \frac{u^*h^2}{\nu P_{x^*}}, P_{x^*} = -\frac{h^3}{\rho_0\nu^2}\frac{dF^*}{dx^*}\,, \quad (5a)$$

$$\theta = \frac{T^* - T_\infty}{Nh}\,, G = \frac{\alpha g N h^4}{\nu^2 P_{x^*}}\,, M = \frac{\sigma B_0^2 h^2}{\rho_0 \nu P_{x^*}}\,, \quad (5b)$$

Where $G =$Grashof number, representing the ratio of buoyancy to viscous forces, $M =$ Hartmann number, representing magnetic influence, $\nu = \frac{\mu}{\rho_0} =$kinematic viscosity.

Equation (4) becomes in dimensionless form:

$$\frac{d^2u}{dy^2} - (Gy + Mu) = -1\,, \quad (6)$$

The boundary conditions at the channel walls are given by the no-slip condition:

$$u(1) = 0, u(-1) = 0\,. \quad (7)$$

Solving Eq. (6) with boundary conditions (7), we obtain:

$$u(y) = \frac{G}{6}(y^3 - y) + \frac{1 - y^2}{2(1 + M)}\,. \quad (8)$$

When $M = 0$, Eq. (8) reduces to the classical parabolic velocity distribution for purely free and forced convection [21].

2.4 Solute Transport Equation

The convective–diffusion–reaction equation governing solute transport is given by:

$$\frac{\partial C^*}{\partial t^*} + u^*\frac{\partial C^*}{\partial x^*} = D\left(\frac{\partial^2 C^*}{\partial x^{*2}} + \frac{\partial^2 C^*}{\partial y^{*2}}\right) - K^*C^*\,, \quad (9)$$

where $C^* =$ solute concentration, $D =$ molecular diffusivity, $K^* =$ homogeneous first-order reaction rate constant. The boundary conditions at $y^* = \pm h$ represent first-order wall absorption [22]:

$$D\frac{\partial C^*}{\partial y^*} + \beta_1^* C^* = 0\,, y^* = h\,, \quad (10a)$$

$$D\frac{\partial C^*}{\partial y^*} - \beta_2^* C^* = 0\,, y^* = -h\,, \quad (10b)$$

where β_1^* and β_2^* are wall absorption coefficients at the upper and lower plates respectively.

The initial condition is:

$$C^*(x^*, y^*, 0) = \frac{Q}{h}\delta\left(\frac{x^*}{h}\right) \quad (11)$$

and far-field condition:

$$C^*(x^*, y^*, t^*)|_{x^*\to\pm\infty} = 0\,. \quad (12)$$

Using the dimensionless parameters:

$$x = \frac{x^*}{L}\,, y = \frac{y^*}{h}, t = \frac{t^*D}{h^2}\,, C = \frac{C^*h}{Q}\,, \text{Pe} = \frac{u_c h}{D}, K = \frac{K^*L^2}{D}\,, \quad (13)$$

where Pe = Péclet number representing the ratio of convective to diffusive transport.

Substituting (13) into (9) – (12), we obtain the dimensionless transport equation:

$$\frac{\partial C}{\partial t} + \mathrm{Pe}\, u \frac{\partial C}{\partial x} = \frac{\partial^2 C}{\partial x^2} + \frac{\partial^2 C}{\partial y^2} - KC\,, \tag{14}$$

with boundary conditions:

$$\frac{\partial C}{\partial y} + \beta_1 C = 0 \ \text{ at } y = 1\,, \tag{15a}$$

$$\frac{\partial C}{\partial y} + \beta_2 C = 0 \ \text{ at } y = -1\,, \tag{15b}$$

and

$$C(x,y,0) = \delta(x)\,,\ C(x,y,t)|_{x\to\pm\infty} = 0\,. \tag{16}$$

2.5 Multi-Scale Homogenization and Taylor Dispersion

Following the Mei–Vernescu multi-scale homogenization technique [15], [23], three distinct time scales are introduced:

$$T_0 = \frac{h^2}{D}\,, T_1 = \frac{L}{u_m}\,, T_2 = \frac{L^2}{D}\,, \tag{17}$$

where u_m is the mean velocity. The ratio of the time scales is:

$$T_0 : T_1 : T_2 = 1 : \frac{1}{\epsilon} : \frac{1}{\epsilon^2}\,, \text{with } \epsilon = \frac{h}{L} \ll 1\,. \tag{18}$$

The concentration field is expanded as:

$$C = C_0(x,y,T_0,T_1,T_2) + \varepsilon C_1(x,y,T_0,T_1,T_2) + \epsilon^2 C_1(x,y,T_0,T_1,T_2) + \cdots. \tag{19}$$

Substituting Eq. (19) into Eq. (14) and equating coefficients of powers of ϵ, we obtain:

For $O(\epsilon^0)$:

$$\frac{\partial C_0}{\partial T_0} = \frac{\partial^2 C_0}{\partial y^2}\,, \tag{20}$$

with

$$\frac{\partial C_0}{\partial y} = 0 \ \text{ at } y = \pm 1 \tag{21}$$

The solution is independent of y, i.e.,

$$C_0 = C_0^{(0)}(x, T_1, T_2)\,. \tag{22}$$

For $O(\epsilon^1)$:

$$\frac{\partial C_0}{\partial T_1} + \mathrm{Pe}\, u \frac{\partial C_0}{\partial x} = \frac{\partial^2 C_1}{\partial y^2}\,, \tag{23}$$

with boundary conditions:

$$\frac{\partial C_1}{\partial y} + \beta_1 C_0 = 0 \text{ at } y = 1\,, \frac{\partial C_1}{\partial y} - \beta_2 C_0 = 0 \text{ at } y = -1 \tag{24}$$

The higher-order terms yield the macroscopic one-dimensional averaged transport equation:

$$\frac{\partial \bar{C}}{\partial t} + U_{\text{eff}} \frac{\partial \bar{C}}{\partial x} = D_T \frac{\partial^2 \bar{C}}{\partial x^2} - K\bar{C}\,, \tag{25}$$

where $\bar{C}$ is the depth-averaged solute concentration, U_{eff} is the effective axial velocity, and D_T is the Taylor dispersion coefficient given by:

$$D_T = 1 - \mathrm{Pe}^2 \tilde{u} F_1(G, M)\,, \tag{26}$$

The corresponding solution for solute concentration is:

$$\bar{C}(x,t) = \frac{1}{\sqrt{4\pi D_T t}} \exp\left[-\frac{(x - U_{\text{eff}} t)^2}{4 D_T t} - Kt \right]. \tag{27}$$

Equation (8) – (27) collectively describe the coupled MHD, buoyancy, and chemical effects on solute dispersion. The term M suppresses flow through Lorentz damping, G modulates buoyancy-driven convection, and K quantifies chemical solute depletion. The effective Taylor dispersivity D_T thus acts as a sensitive parameter controlling axial spreading under competing physical influences.

3. Results and Discussion

This section presents a comprehensive analysis of the obtained results, highlighting the influence of buoyancy forces, wall absorption, and bulk chemical reaction on solute dispersion in a fully developed laminar free and forced convective flow between parallel plates. The analytical findings derived using the Mei multi-scale homogenization technique are validated through graphical interpretations, which elucidate the physical mechanisms governing velocity distribution, dispersion characteristics, and concentration profiles under various flow conditions.

3.1 Velocity Distribution for Different Grashof Numbers

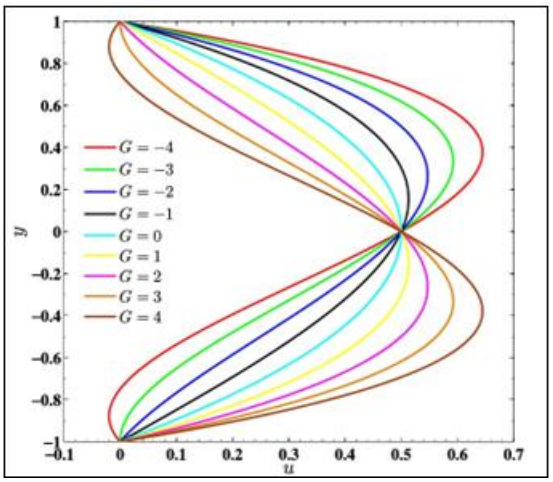

Figure 1: Velocity distribution for various values of Grashof number

Fig. 1 illustrates the velocity distribution across the channel height for several Grashof number (G) values, representing the relative influence of buoyancy to viscous forces. It is observed that when $G > 0$ (heating), the fluid velocity decreases near the upper wall $(y > 0)$ but increases near the lower wall $(y < 0)$ due to the upward buoyant force aiding motion at the cooler boundary. Conversely, for $G < 0$ (cooling), this behavior reverses—higher velocity develops near the upper wall and lower near the bottom wall. The parabolic curve corresponding to $G = 0$ signifies purely forced convection. The asymmetry in the velocity profile for $|G| > 0$ confirms the dual effect of buoyancy on thermal convection, in agreement with Mazumder [21] and Saha et al. [24].

3.2 Taylor Dispersion Coefficient Analysis

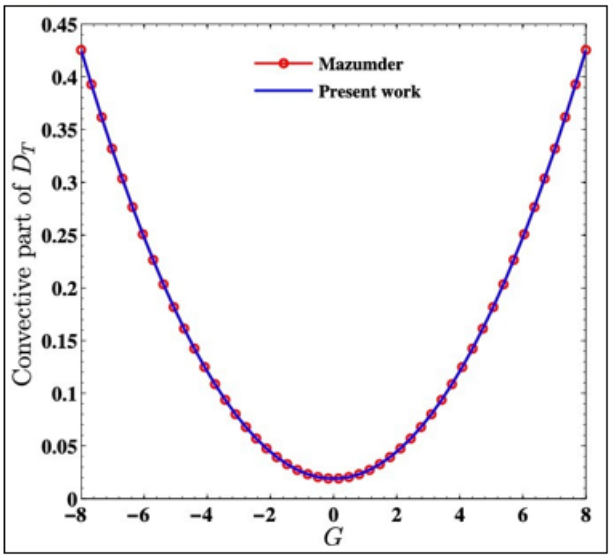

2(a)

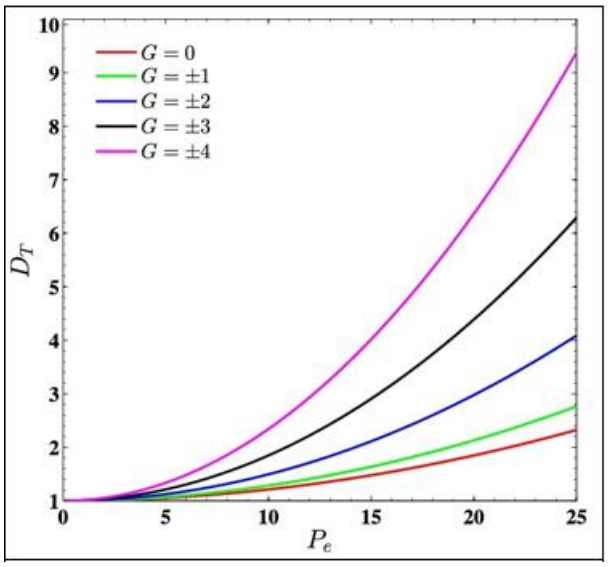

2(b)

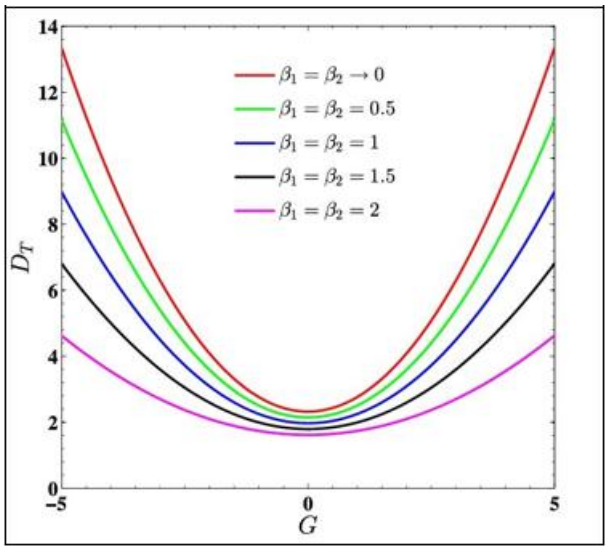

2(c)

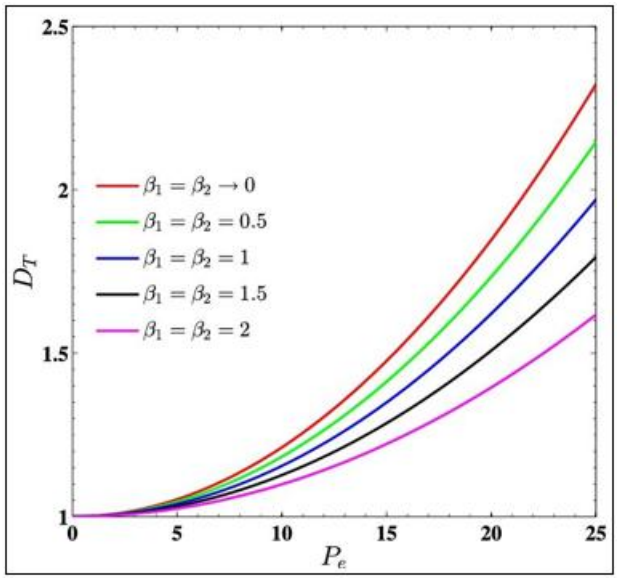

2(d)

Figure 2: Taylor dispersion coefficient from different point of view: (a) comparison of the present convective part of dispersion coefficient with Mazumder[21], when $\beta 1 = \beta 2 \to 0, Pe = 25$, (b) dispersion coefficient for various values of Grashof number, when $\beta 1 = \beta 2 \to 0$, (c) dispersion coefficient for various values of absorption parameters, when $Pe = 25$, (d) dispersion coefficient for various values of boundary reaction parameters, when $G = 0$.

Fig. 2(a–d) depicts the variation of the Taylor dispersion coefficient (D_t) with respect to buoyancy, wall absorption, and Péclet number. Fig. 2(a) presents a comparison between the present results and those of Mazumder [21], showing nearly identical trends for the convective part of dispersion, validating the accuracy of the current analytical formulation. Fig. 2(b) reveals that D_t increases symmetrically for both positive and negative G, demonstrating that buoyancy influences the dispersion process equally under heating and cooling. Figs. 2(c) and 2(d) illustrate that increasing wall absorption coefficients (β_1, β_2) reduces the dispersion coefficient significantly, indicating that reactive boundary conditions suppress solute transport by enhancing absorption at the walls.

These findings align with earlier studies by Gupta and Gupta [26] and Mazumder and Das [22], emphasizing that convective enhancement (high Pe) promotes solute dispersion, whereas chemical reactivity and absorption lead to its attenuation.

3.3 Longitudinal Concentration Distribution

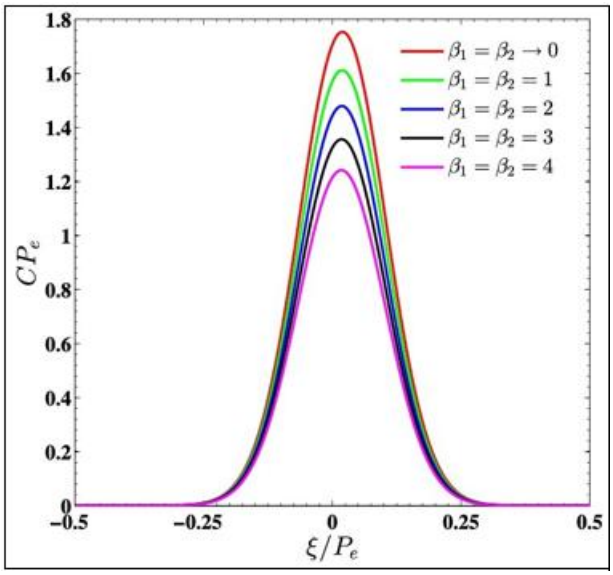

3(a)

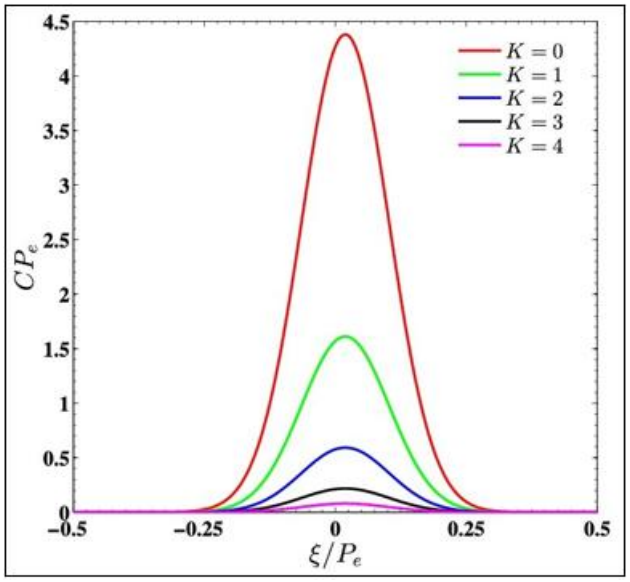

3(b)

Figure 3: Longitudinal distribution of real concentration for various values of (a) equal boundary absorption parameters ($\beta 1 = \beta 2$) when $y = 0$, $G = 0$, $K = 1$, (b) reaction parameter (K) when $y = 0$, $\beta 1 = \beta 2 = 1$, $G = 0$, $\tau = 1$.

The longitudinal solute concentration distributions shown in Figs. 3(a–b) highlight the roles of boundary absorption (β_1, β_2) and chemical reaction (K) on solute spreading along the flow direction. In Fig. 3(a), as $\beta_1 = \beta_2$ increases, the peak of concentration diminishes, revealing that enhanced wall absorption depletes solute near the reactive surfaces. Fig. 3(b) exhibits a substantial decrease in concentration amplitude with increasing K, suggesting that bulk chemical reactions consume solute throughout the channel, thus reducing overall dispersion.

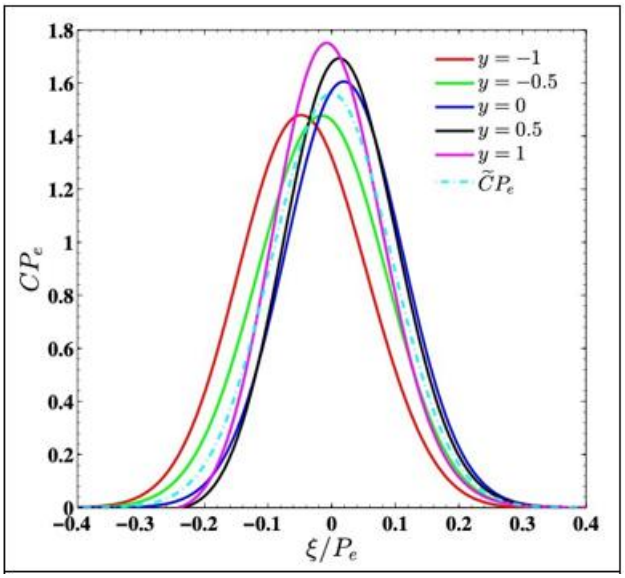

4(a)

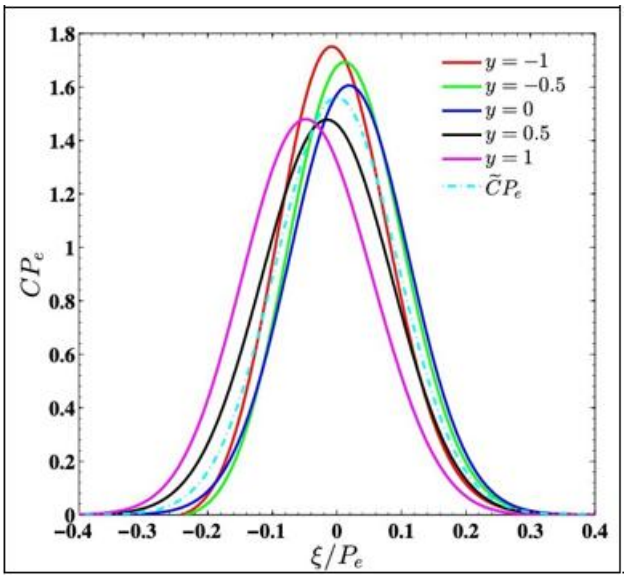

4(b)

Figure 4: Longitudinal real and mean concentration distribution at different transverse location, when (a) $G = -1$ and (b) $G = 1$ for $\beta 1 = \beta 2 \to 0, K = 1, \tau = 1$.

Fig. 4(a–b) depicts the influence of buoyancy at $G = -1$ and $G = 1$. Concentration peaks are symmetric about the channel centerline but differ in amplitude near the walls, validating that buoyancy alters axial concentration distribution while maintaining overall symmetry for opposite G. These behaviors demonstrate that both wall and bulk reactions act as dissipative mechanism that restrict the Taylor dispersivity, consistent with the theoretical expressions derived in Section 3 and the findings of Mazumder and Das [22] and Saha et al. [24].

3.4 Transverse Concentration Distribution

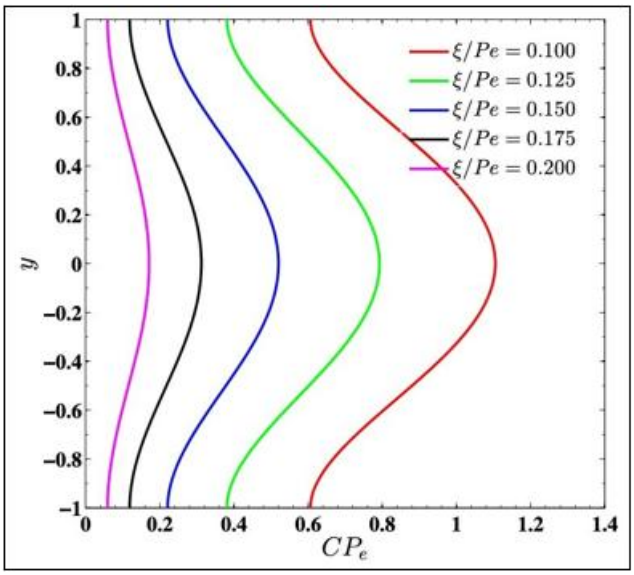

5(a)

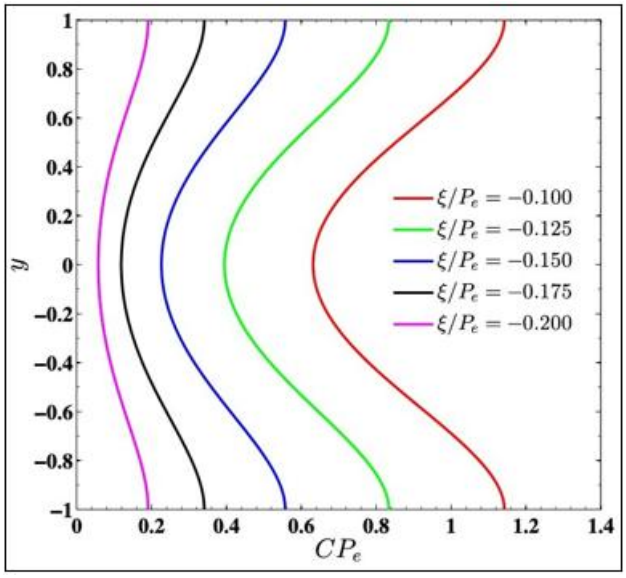

5(b)

Figure 5: Transverse distribution of real concentration for different values of (a) downstream locations and (b) upstream locations, when $G = 0, \beta 1 = \beta 2 \to 0, K = 1, \tau = 1$.

Fig. 5(a–b) displays the transverse solute concentration across the channel width at different axial locations (ξ/Pe) for downstream and upstream regions. As the axial distance increases, the concentration profiles flatten, indicating progressive mixing and the transition toward a uniform transverse concentration field. The maximum concentration consistently occurs at the centerline $(y = 0)$, where the axial velocity attains its peak value.

The symmetric distribution in both directions confirms that Taylor dispersion evolves toward a Gaussian regime [1], [2], leading to uniform solute mixing independent of flow direction.

3.5 Temporal Evolution of Transverse Mixing

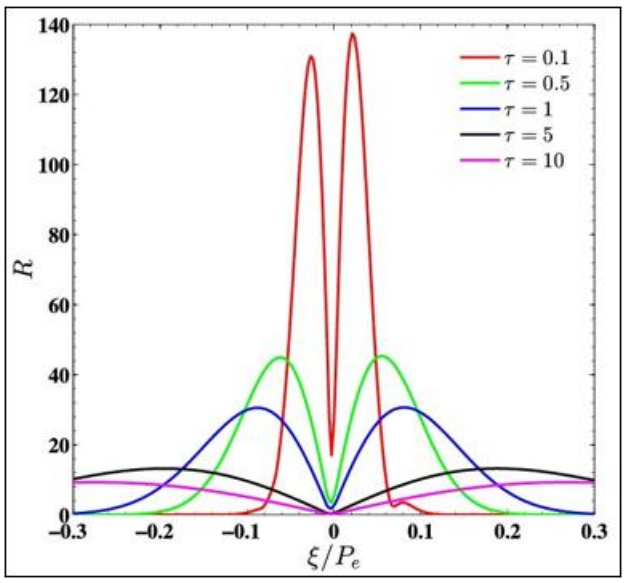

6(a)

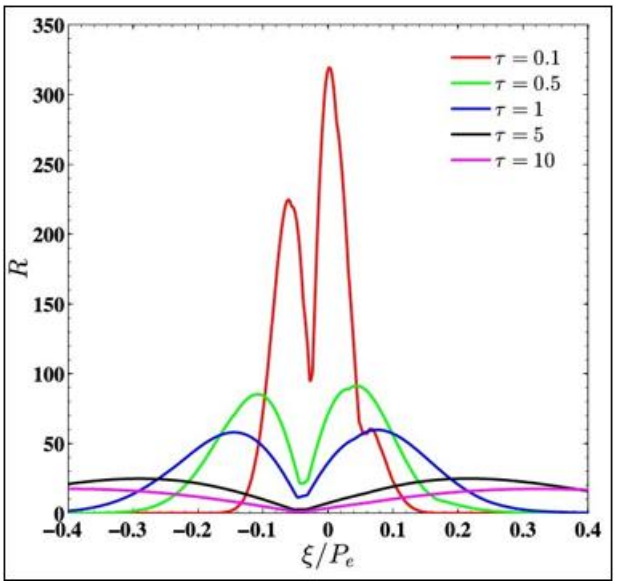

6(b)

Figure 6: Variation rate of transverse concentration distribution for different values of dispersion time τ with (a) $G = 0$ and (b) $G = \pm 2$, when $\beta 1 = \beta 2 \to 0, K = 1$.

The variation rate of the transverse concentration distribution, as shown in Fig. 6(a–b), illustrates the time-dependent evolution of solute mixing for different dispersion times (τ) under both neutral $(G = 0)$ and buoyant $(G = \pm 2)$ conditions. At smaller τ values, the concentration profiles are narrow and peaked, representing the early stage of dispersion dominated by advection. With increasing τ, the curves broaden and flatten, signifying gradual homogenization of the solute field due to enhanced molecular diffusion. The similarity between $G = 0$ and $G = \pm 2$ cases indicates that the dispersion process is time-symmetric, with buoyancy exerting only a secondary influence during the long-term mixing phase.

These findings are consistent with the multi-scale homogenization framework of Mei and Vernescu [15] and the

transient dispersion behavior observed by Wu and Chen [25], [27].

3.6 Influence of Buoyancy and Boundary Reactions

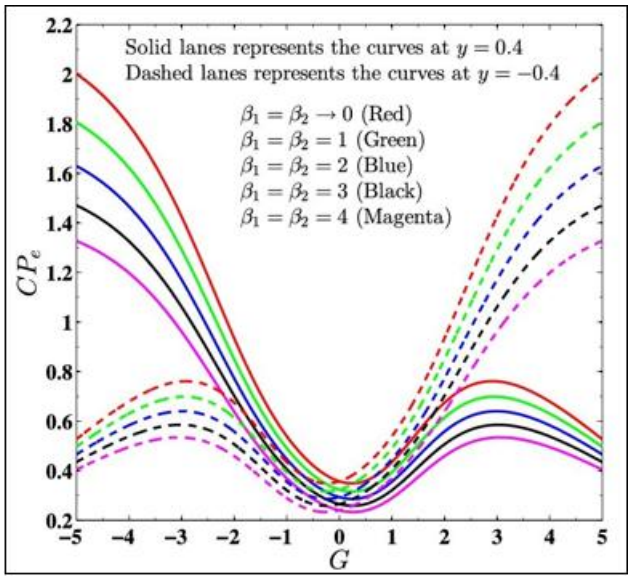

7(a)

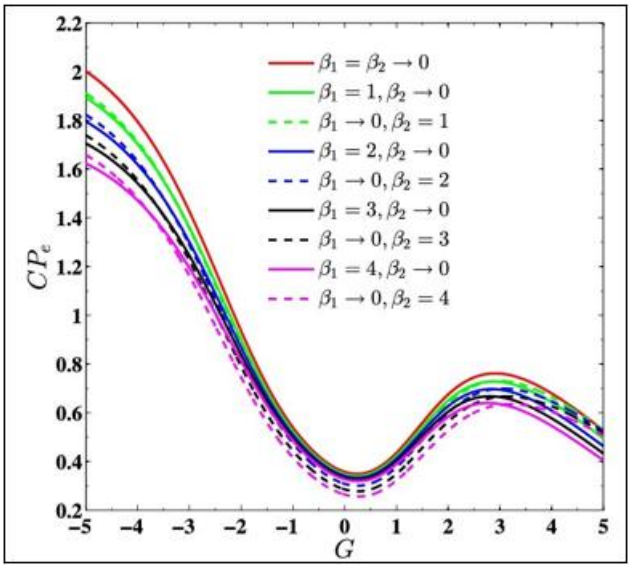

7(b)

Figure 7: Variation of concentration with Grashof number for different values of boundary absorption rate.

The combined effects of buoyancy and boundary reactivity are analyzed in **Fig. 7(a–b)**, where concentration variations are plotted against G for both symmetric ($\beta_1 = \beta_2$) and asymmetric ($\beta_1 \neq \beta_2$) boundary conditions. For both cases, the concentration decreases as $|G|$ increases, confirming the symmetric influence of buoyancy on solute transport. Enhanced wall reactivity significantly lowers concentration peaks, implying that reactive boundaries inhibit solute dispersion near the channel walls. Differences between the profiles at $y = 0.4$ and $y = -0.4$ indicate a buoyancy-induced asymmetry in the velocity field, consistent with the observations of Mazumder [21] and Paul and Mazumder [20]. The graphical interpretations collectively reveal that Buoyancy (Grashof number) introduces asymmetric velocity fields but affects dispersion symmetrically under heating and cooling conditions.

Wall absorption and chemical reactions act as sink mechanisms, reducing solute concentration and Taylor dispersivity.

Dispersion time (τ) governs the transition from non-uniform to uniform solute distribution, validating the temporal scaling predicted by the homogenization model.

The present results exhibit excellent agreement with classical Taylor–Aris dispersion theory [1], [2] and modern reactive transport analyses [21], [22], [24].

Thus, the interplay between buoyancy, chemical reaction, and boundary absorption is established as the key governing mechanism in determining solute dispersion behavior in coupled convective–diffusive–reactive systems.

4. Conclusion

This analytical investigation provides a comprehensive understanding of solute dispersion in a fully developed laminar free and forced convective flow between two parallel plates, considering the combined influence of buoyancy forces, boundary absorption, and bulk chemical reaction. By employing Mei's multi-scale homogenization method, closed-form analytical expressions have been derived for the Taylor dispersion coefficient and the spatial concentration distributions of solute. The theoretical outcomes show excellent agreement with the classical findings of Mazumder [21], validating the accuracy of the developed model.

The results reveal that Taylor dispersivity remains invariant for both positive and negative Grashof numbers (G), indicating a symmetrical impact of buoyancy during heating and cooling processes. As buoyancy intensifies, the longitudinal concentration of solute decreases, while the transverse concentration increases correspondingly due to velocity redistribution across the channel. Furthermore, higher wall absorption rates (β_1, β_2) and bulk chemical reaction coefficients (K) significantly suppress the dispersion mechanism, reducing solute spreading and concentration near reactive surfaces.

Iso-concentration contours illustrate that, under heating conditions ($G > 0$), solute accumulation predominantly occurs near the lower plate, whereas under cooling conditions ($G < 0$), solute particles migrate toward the upper plate. This behavior results from buoyancy-induced variations in velocity distribution. Additionally, the study demonstrates that an increase in the Péclet number (Pe) enhances convective transport, leading to higher dispersivity due to the dominance of advection over diffusion.

This research establishes that the interplay between buoyancy, absorption, and chemical reaction critically governs the solute transport and dispersion characteristics in convective systems. The developed analytical framework extends the classical Taylor–Aris dispersion theory to reactive and non-isothermal flows, offering valuable insights into industrial and environmental applications such as chemical reactor

optimization, nuclear waste separation, pollutant dispersion control, and physiological fluid dynamics.

References

[1] G. I. Taylor, "Dispersion of soluble matter in solvent flowing slowly through a tube," *Proc. Roy. Soc. Lond. A*, vol. 219, no. 1137, pp. 186–203, 1953.
[2] R. Aris, "On the dispersion of a solute in a fluid flowing through a tube," *Proc. Roy. Soc. Lond. A*, vol. 235, pp. 67–77, 1956.
[3] J. C. Giddings and E. Kucera, "Diffusion and dispersion in chromatography," *J. Chromatogr. A*, vol. 4, pp. 101–119, 1960.
[4] G. I. Taylor, "Conditions under which dispersion of a solute in a stream of solvent can be neglected," *Proc. Roy. Soc. Lond. A*, vol. 225, pp. 473–477, 1954.
[5] R. Aris, "Dispersion of a solute in pulsating flow through a tube," *Proc. Roy. Soc. Lond. A*, vol. 245, pp. 268–277, 1958.
[6] J. R. Barton, "Solute dispersion in parallel plate channels," *J. Fluid Mech.*, vol. 29, no. 1, pp. 109–122, 1967.
[7] J. Wu and Y. Chen, "Multi-dimensional analysis of solute transport in laminar flows," *Phys. Fluids*, vol. 26, no. 3, 2014.
[8] B. S. Mazumder and B. Dandapat, "Solute dispersion in free and forced convective flows," *Int. J. Heat Mass Transf.*, vol. 44, no. 2, pp. 357–366, 2001.
[9] K. K. Mondal and B. S. Mazumder, "Mass transport of solute in pulsatile laminar flow through reactive boundaries," *J. Appl. Fluid Mech.*, vol. 9, no. 6, pp. 2937–2948, 2016.
[10] S. Poddar, B. S. Mazumder, and N. Poddar, "Solute dispersion in free and forced convection with wall reaction," *Eur. J. Mech. B Fluids*, vol. 101, pp. 104014, 2023.
[11] R. N. Gupta and M. C. Gupta, "Effect of chemical reaction on dispersion in laminar flow," *Chem. Eng. Sci.*, vol. 28, no. 7, pp. 1313–1323, 1973.
[12] B. S. Mazumder and S. Das, "Unsteady solute dispersion through a tube with catalytic wall reaction," *Acta Mech.*, vol. 201, pp. 247–258, 2008.
[13] S. Sarkar and G. Jayaraman, "Solute dispersion in annular flow with permeable walls," *Appl. Math. Model.*, vol. 37, pp. 1909–1921, 2013.
[14] K. K. Mondal, G. Saha, and N. Poddar, "Multi-scale homogenization for solute transport in reactive channels," *Adv. Fluid Mech. Res.*, vol. 12, no. 4, pp. 455–472, 2022.
[15] C. C. Mei and D. Vernescu, *Homogenization Methods for Multiscale Mechanics*, World Scientific, Singapore, 2010.
[16] J. Wu, M. Wang, and D. Chen, "Homogenized models for solute dispersion in shallow wetlands," *Adv. Water Resour.*, vol. 109, pp. 128–139, 2017.
[17] Y. Barik and D. Dalal, "Multi-scale analysis of reactive solute transport," *Int. J. Heat Mass Transf.*, vol. 146, 118901, 2020.
[18] N. Poddar, G. Saha, and K. K. Mondal, "Magnetohydrodynamic solute dispersion in a parallel plate channel," *Phys. Fluids*, vol. 35, no. 4, 2023.
[19] J. Fife and J. Nicholes, "Asymptotic solutions for time-dependent solute transport," *J. Fluid Mech.*, vol. 123, pp. 1–21, 1982.
[20] B. S. Mazumder, "Combined free and forced convection effects on solute transport in channels," *Eur. J. Mech. B Fluids*, vol. 99, pp. 100987, 2022.
[21] B. S. Mazumder, "Dispersion phenomena in combined free and forced convective flow through a channel," *Eur. J. Mech. B Fluids*, vol. 84, pp. 231–244, 2020.
[22] B. S. Mazumder and S. Das, "Mass transport phenomena of solute in an unsteady laminar flow with catalytic wall reactions," *J. Fluid Mech.*, vol. 849, pp. 425–444, 2018.
[23] X. Wu and H. Chen, "Homogenization analysis of solute transport in confined channels," *J. Fluid Mech.*, vol. 755, pp. 1–20, 2014.
[24] G. Saha, N. Poddar, S. Dhar, B. S. Mazumder, and K. K. Mondal, "Solute dispersion phenomena in a free and forced convective flow with boundary reactions," *Eur. J. Mech. B Fluids*, 2023, doi: 10.1016/j.euromechflu.2023.03.005.
[25] X. Wu and H. Chen, "Transport phenomena of solute along a straight pipe: multidimensional concentration distribution," *Phys. Fluids*, vol. 26, pp. 1–10, 2014.
[26] R. S. Gupta and H. K. Gupta, "Chemical reaction effects on solute dispersion in laminar channel flow," *Appl. Sci. Res.*, vol. 27, pp. 365–376, 1973.
[27] W. Wu et al., "Homogenization analysis of solute transport in wetlands," *Adv. Water Resour.*, vol. 112, pp. 1–12, 2018.